*International Journal of Thermophysics, Vol. 25, No. 2, March 2004 (© 2004)*

# A Transient Method for Total Emissivity Determination[1]

**B. Zhang,[2,3] J. Redgrove,[2] and J. Clark[2]**

A transient method for determining the hemispherical total emissivity of solids is investigated using an emissometer recently developed at the NPL. The emissivity is calculated from measurement of the sample surface temperature coupled with a knowledge of its bulk thermal properties. This was conducted as part of the current work to validate the new NPL apparatus for high temperature emissivity measurements. A theoretical study shows that when a thermally thick sample is allowed to radiate instantaneously into a cold environment, then the resulting transient surface temperature depends solely on its hemispherical total emissivity and effusivity. This approach is used to obtain a hemispherical total emissivity value for Fecralloy steel, and it is then compared with the normal total emissivity value obtained by integration of normal spectral emissivity measurements in the wavelength range 2 to 9 μm.

**KEY WORDS:** Fourier transform spectrometer; hemispherical total emissivity; high temperature.

## 1. INTRODUCTION

Conventional techniques for measuring the hemispherical total emissivity include the direct-heating method where a dc current is allowed to pass through a metallic sample and the emissivity is determined from the measured surface temperature and area, and electrical power lost by radiation from its surface [1]. This is the calorimetric method. For nonmetallic materials that cannot be electrically self-heated, the emissivity can be

[1] Paper presented at the Fifteenth Symposium on Thermophysical Properties, June 22–27, 2003, Boulder, Colorado, U.S.A.

[2] Centre for Basic, Thermal and Length Metrology, National Physical Laboratory, Queens Road, Teddington, Middlesex TW11 0LW, United Kingdom.

[3] To whom correspondence should be addressed. E-mail: bufa.zhang@npl.co.uk



0195-928X/04/0300-0423/0 © 2004 Plenum Publishing Corporation

calculated by integrating angular spectral emissivity values measured using a radiometric method [2]. Use of the Fourier transform spectrometer (FTS) makes radiometric total emissivity evaluation much easier and more accurate since an FTS can measure radiation over a wide range of wavelengths with high spectral resolution [3–5]. Measurements at angles to the sample surface need to be performed for calculating the hemispherical total emissivity of the sample.

A main source of uncertainty in steady-state emissivity measurement methods is surface temperature measurement. To overcome this difficulty, a transient technique has been developed at the NPL [6] in which the sample is first heated to a steady, uniform temperature in a furnace and a plane surface of the sample is then rapidly exposed to a cold environment and begins to radiate freely, during which time its thermal spectral radiation signal is measured and recorded. To reduce the measurement uncertainty caused by the limited exposure speed, the recorded transient data are fitted to a theoretical model to allow extrapolation of the data back to time "zero," corresponding to the initial isothermal condition. This allows accurate determination of target radiation at the initial isothermal temperature and thus, following a blackbody measurement, an accurate sample emissivity value.

A new NPL emissometer has been developed recently which uses a Fourier transform spectrometer to expand the ranges of temperature and wavelength, and which has a periscope to allow angular measurements at angles of up to 70° from normal to the sample surface. The hemispherical total emissivity can be calculated by integrating angular spectral emissivity values [7].

The work presented here was conducted as part of the validation of the new apparatus for high temperature emissivity measurements. The aim was to determine the hemispherical total emissivity of the sample by monitoring its surface temperature and applying the theoretical solution for a freely radiating semi-infinite solid, and to compare that with the emissivity value obtained independently by integration of normal spectral emissivity measurements.

## 2. METHOD

During a transient emissivity measurement in vacuum, heat is lost from the sample surface by thermal radiation. If the sample is assumed to be homogeneous, isotropic, optically opaque, and thermally wide and thick enough, then, for modeling purposes, it can be considered as a semi-infinite solid. Also, assuming that the emissivity is unchanged during the measurement—emissivity is usually a weak function of temperature and the

temperature change during measurement is small—then the changing sample surface temperature can be calculated from the measured radiation signal. A theoretical model can be used to estimate the uncertainty caused by the limited sample exposure speed—by fitting the measurement signal to the model and extrapolating the fit to $t = 0$, the time at which the sample is at its initial isothermal temperature [6].

The surface temperature of a semi-infinite sample with surface radiation cooling has been studied by Jaeger [8], and this forms the basis of the method we have adopted here for estimation of the hemispherical total emissivity. By taking a co-ordinate system with $x = 0$ at the sample surface and positive inside, its temperature field, $T(x, t)$, can be described by Fourier's equation as follows:

$$\frac{\partial^2 T}{\partial x^2} = \frac{1}{\alpha}\frac{\partial T}{\partial t} \tag{1}$$

where $\alpha$ is the thermal diffusivity of the sample, together with $T(x, 0) = T_0$ for $x \geqslant 0$ for the initial condition where $T_0$ is the initial ($t = 0$) temperature of the sample. The radiation heat flux, $q(t)$, at its surface ($x = 0$) is $q(t) = \varepsilon\sigma(T_S^4 - T_a^4)$, where $T_S(t) = T(0, t)$ is the sample surface temperature. $T_a$ is the temperature of the environment to which the sample surface radiates, $\varepsilon$ is the hemispherical total emissivity of the sample, and $\sigma = 5.67 \times 10^{-8}$ $\mathrm{W \cdot m^{-2} \cdot K^{-4}}$ is the Stefan–Boltzmann constant.

For continuity of heat flow, the condition $q(t) = \kappa \frac{\partial T}{\partial x}$ at $x = 0$ also applies, where $\kappa$ is the thermal conductivity of the sample. The solution for Eq. (1) with the above boundary conditions can be calculated and the sample surface temperature $T_S(t)$ is given by (see Appendix A)

$$T_S(t) = T_0\left(1 + \sum_{n=1}^{\infty} \frac{a_n}{n!}\left(\frac{t}{t_0}\right)^{\frac{n}{2}}\right) \tag{2}$$

for $t > 0$, where

$$t_0 = \frac{p^2}{\varepsilon^2\sigma^2 T_0^6} \tag{3}$$

is a specific time related to the sample's thermal properties and the initial sample temperature, $T_0$. The term $p = \sqrt{\kappa\rho C_p}$ is the effusivity of the material, and $\rho$ and $C_p$ are the density and specific heat capacity, respectively, linking thermal conductivity $\kappa$ and diffusivity $\alpha$ by $\kappa = \alpha\rho C_p$. The terms $a_n$ become constants when $T_0 \gg T_a$, as discussed in Appendix A.

Equation (2) shows that the decrease in surface temperature is thus solely dependent on $t/t_0$.

Once the surface temperature has been calculated, the thermal radiative heat flux at the sample surface can be evaluated and expressed in the form of a Taylor series as follows

$$q(t) = q_0 \left(1 + \sum_{n=1}^{\infty} \frac{b_n}{n!} \left(\frac{t}{t_0}\right)^{\frac{n}{2}}\right) - \left(\frac{T_a}{T_0}\right)^4 q_0 \tag{4}$$

for $t > 0$, where $q_0 = \varepsilon\sigma T_0^4$ and the $b_n$ coefficients are as given in Appendix A.

Using Planck's radiation law, and assuming negligible background radiation (which is a reasonable assumption at elevated temperatures, as illustrated by Figs. 1 and 2), the measured spectral radiation signal from the sample surface is given by

$$S(\lambda, t) = S_0(\lambda) \frac{e^{\frac{C_2}{\lambda T_0}} - 1}{e^{\frac{C_2}{\lambda T_S}} - 1} \tag{5}$$

for $t > 0$, where $S_0(\lambda)$ is the initial measured spectral radiation signal at wavelength $\lambda$, and $C_2 = 14388\ \mu\text{m}\cdot\text{K}$ is the second radiation constant. For the purpose of curve fitting to measured data, using Eq. (2) for $T_S$ and expanding Eq. (5) as a Taylor series in $(t/t_0)^{1/2}$ (see Appendix A), gives

$$S(\lambda, t) = S_0(\lambda) \left(1 + \sum_{n=1}^{\infty} \frac{d_n}{n!} \left(\frac{t}{t_0}\right)^{\frac{n}{2}}\right) \tag{6}$$

Equation (6) shows that the spectral radiation signal is dependent on $t_0$ and $d_n$, where $d_n$ in turn is dependent on the parameters $T_a/T_0$ and $\lambda T_0$.

Calculations have been performed to evaluate the changes with time of the sample surface temperature, heat flux, and spectral signals. Equations (2), (4), and (6) show that, when normalized by their initial values at $t = 0$, those quantities can be studied in a dimensionless time scale, $t/t_0$, and therefore become independent of the sample thermal properties.

For small $t/t_0$, Eqs. (2), (4), and (6) are rapidly convergent and only a few of the $a_n$, $b_n$, and $d_n$ values need to be computed. For example, for $t/t_0 < 0.01$, the computation error is less than 1.2% due to taking only the first two $a_n$ values, less than 0.53% with three $a_n$ values, less than 0.33% with four $a_n$ values, and so on. The effect on the sample surface caused by the measurement environment being at temperatures above 0 K are considered in (a) to (c) below.

(a) Surface temperature: Figure 1 shows surface temperature calculations where the initial temperature of the sample varies between 400 and 1000 K, and the environment temperatures are 0 and 300 K, respectively. It can be seen that the surface temperature decreases less rapidly when the sample surface is exposed to a 300 K environment than to 0 K. This is because the sample surface absorbs some radiation from the environment when $T_a > 0$ K. The environment temperature has a significant effect on changes in sample surface temperature when it is not much lower than the sample temperature. However, this effect becomes negligibly small when $T_0 \gg T_a$ (for instance, $T_0 =$ 1000 K to $T_a = 300$ K in Fig. 1).

(b) Surface radiative heat flux: Figure 2 shows that the net heat flux from the sample surface can depend strongly on the environment temperature. For example, when $T_0 = 400$ K, the flux is 30% less for $T_a = 300$ K than for $T_a = 0$ K. The flux difference decreases as the temperature difference between the sample and environment increases.

(c) Spectral radiation signal: Spectral radiation signals are calculated in Fig. 3 to show that they change with time in a similar way to those for the surface temperature, but at greater rates. The signals depend on environment temperature and, more significantly, on wavelength.

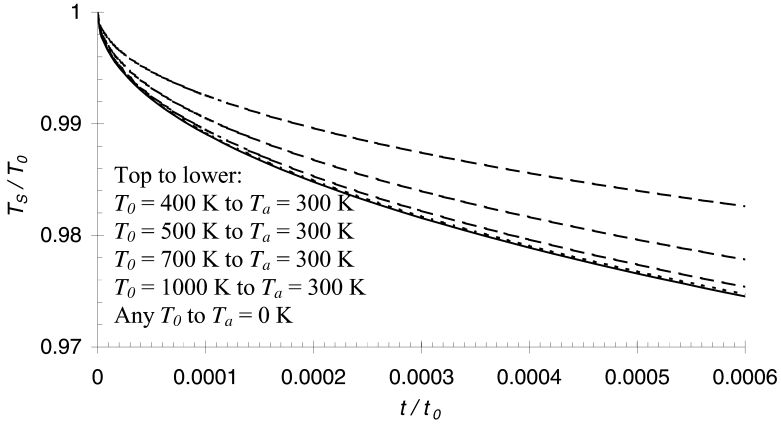


**Fig. 1.** Theoretical calculation of sample surface temperature versus time for radiation from the surface into an environment at 300 K (dashed lines) and 0 K (solid line).

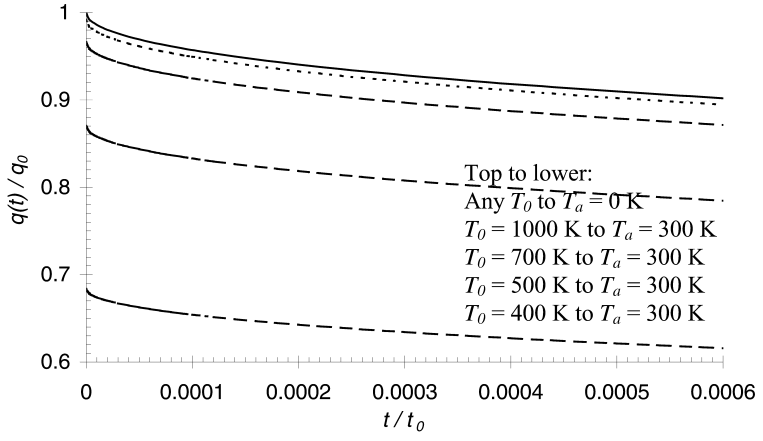


**Fig. 2.** Theoretical calculation of surface radiative heat flux versus time.

## 3. APPARATUS

Figure 4 shows the new NPL apparatus. Within the vacuum chamber are four main parts: a moveable tantalum heating furnace, graphite sample block, high-speed shutter, and periscope for viewing the detected area at prescribed angles. A computer controls the shutter motor and performs data analysis on signals acquired from the FTS. The FTS measures radiation from the sample or blackbody cavity obtained via the vacuum chamber periscope and $CaF_2$ window.

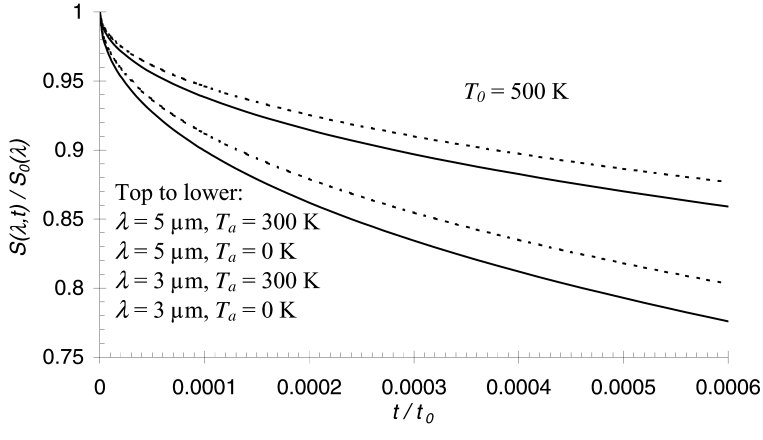


**Fig. 3.** Theoretical calculation of spectral radiation signal versus time.

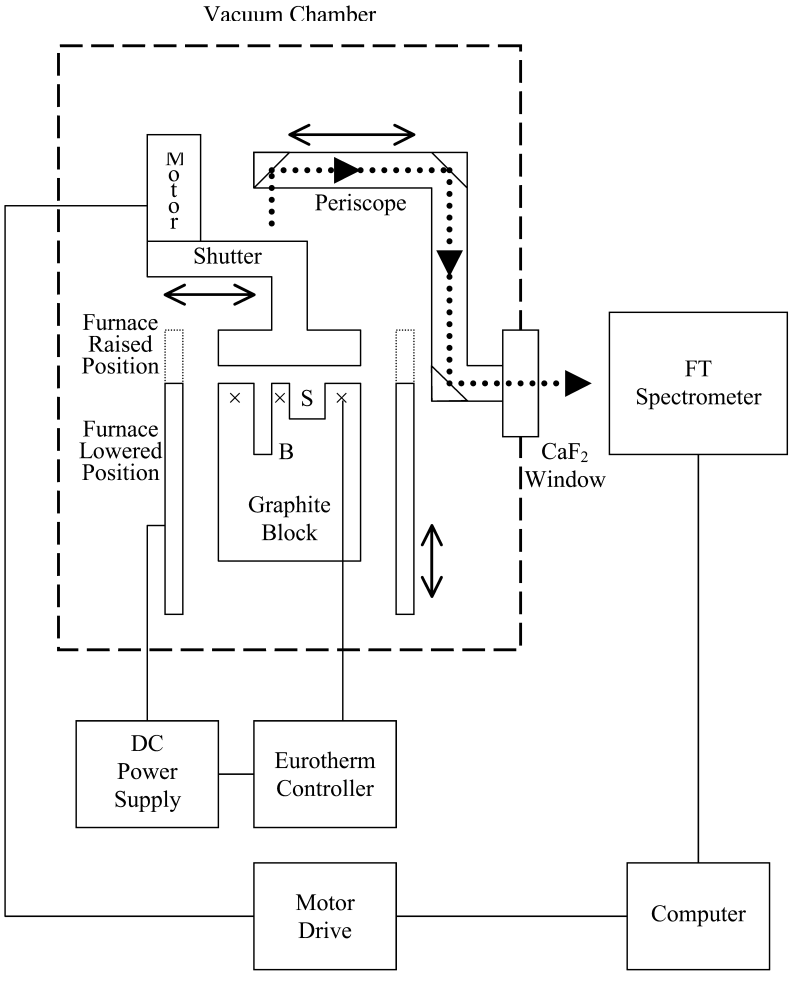


**Fig. 4.** Block diagram of the NPL emissivity apparatus, where three crosses show thermocouple positions inside the graphite block, S is the sample well and B is the blackbody cavity.

The apparatus employs an Equinox 55 FT-IR spectrometer with 16-bit data resolution, supplied by Bruker (UK) Ltd. The spectrometer has a choice of two beam splitters (quartz and Ge/KBr) and three detectors (silicon diode, $LN_2$-cooled InSb, and MCT). The combinations of these beam splitters and detectors ensure that the spectrometer can measure radiation over the wavelength range of 0.6 to 9.6 μm. The upper limit of 9.6 μm is due to the cut-off wavelength of the $CaF_2$ window in the vacuum chamber.

## 4. MEASUREMENTS

### 4.1. Selecting the Sample Measurement Time

For a total emissivity measurement to be successful, it is necessary to satisfy the following two criteria:

(i) $\Delta t$ needs to be controlled so that a sufficiently large dynamic range in measurement signal is possible while avoiding large drops in the sample surface temperature (large temperature changes may lead to a change in sample emissivity, thus violating the assumption made in the theoretical model). For instance, to achieve a temperature drop within 1 to 2%, $\Delta t$ needs to lie between $8.3 \times 10^{-5} t_0$ and $3.5 \times 10^{-4} t_0$ (Fig. 1).

(ii) The measurement time $\Delta t$ is smaller than the heat diffusion time from the sample center to its nearest edge to avoid significant thermal reflection from its boundaries. For example, assuming an instantaneously generated uniform heat impulse along the central axis of an infinite solid at time $t = 0$, then about 8% of the heat is conducted beyond a distance $L$ from the axis by time $t = 0.1 L^2 \alpha^{-1}$. This allows us to set a sample size criterion, applicable to both the diameter and thickness.

To conclude, criteria (i) and (ii) above set limits on the measurement time $\Delta t$ and sample dimensions, respectively.

To estimate $\Delta t$, $t_0$ is calculated with Eq. (3) for some materials using property data shown in Table I. The calculation shows that, for example, to achieve a 1% decrease in the surface temperature for a measurement on Fecralloy steel at $T_0 = 1000$ K, $\Delta t = 22$ s is required (see Fig. 1 for temperature profile and Table I for $t_0$ value). However, to achieve the same 1% drop in surface temperature for Pyroceram 9606 at $T_0 = 2000$ K, the measurement needs to be completed within $\Delta t = 9$ ms. Thus, a much faster measurement speed is required in the latter case. This shows that the evaluation of $t_0$ will help to define $\Delta t$ for a suitable dynamic range of signal. To satisfy criterion (ii), the constraint $L > (10\alpha\, \Delta t)^{1/2}$ must apply. As an example, by taking $\Delta t = 10^{-5} t_0$, the minimum sample size $L_{\min}$ can be calculated by $L_{\min} = (10\alpha\, \Delta t)^{1/2} = 0.01 \kappa \varepsilon^{-1} \sigma^{-1} T_0^{-3}$, that is, $\varepsilon \sigma T_0^4 = 0.01 L_{\min}^{-1} \kappa T_0$, showing that the thermal radiation heat flux from the sample surface is much smaller than that of thermal conduction inside it. For illustration, Fig. 5 shows calculation of the temperature dependence of $L_{\min}$ and $\Delta t$ for materials shown in Table I.

The diameter of the sample in the NPL apparatus is currently limited to 10 mm. (Note: it would be better if the sample size were larger, but the

**Table I.** Calculation of $t_0$ Using Eq. (3) for Various Materials with Thermal Properties from Various Sources

| Material | $T_0$ (K) | $\kappa$ ($W \cdot m^{-1} \cdot K^{-1}$) | $\rho$ ($kg \cdot m^{-3}$) | $C$ ($J \cdot kg^{-1} \cdot K^{-1}$) | $\varepsilon$ | $\alpha$ ($10^{-6} m^2 \cdot s^{-1}$) | $t_0$ ($10^4$ s) |
|---|---|---|---|---|---|---|---|
| Boron nitride (BN) | 1000 | 0.3 | 2250 | 1700 | 0.75 | 0.784 | 0.0635 |
| Fecralloy steel (Fecr) | 1000 | 16 | 7220 | 460 | 0.25 | 4.82 | 26.4 |
| Tantalum (Ta) | 1000 | 60 | 16670 | 152 | 0.2 | 23.7 | 118 |
| Pyroceram 9606 (Pyro) | 2000 | 2.8 | 2600 | 1500 | 0.7 | 0.718 | 0.0108 |
| Silicon (Si) | 2000 | 124 | 2330 | 702 | 1.0 | 75.8 | 0.0986 |
| Tungsten (W) | 2000 | 119 | 19300 | 135 | 0.5 | 45.7 | 0.603 |

current apparatus was not designed for measurement of hemispherical total emissivity by the technique investigated here.) The model applies to a semi-infinite solid and so there is a limited time within which the sample matches the model, i.e., before heat diffuses to the sample boundary. As discussed above, it is also important that there is not a steeply dropping surface temperature. Of the materials listed in Table I the Fecralloy steel best fits these criteria and so it was selected for study.

## 4.2. Experimental Procedure

During an emissivity measurement, a baseline (zero) reading is required to determine signal values and, for this purpose, a few readings are

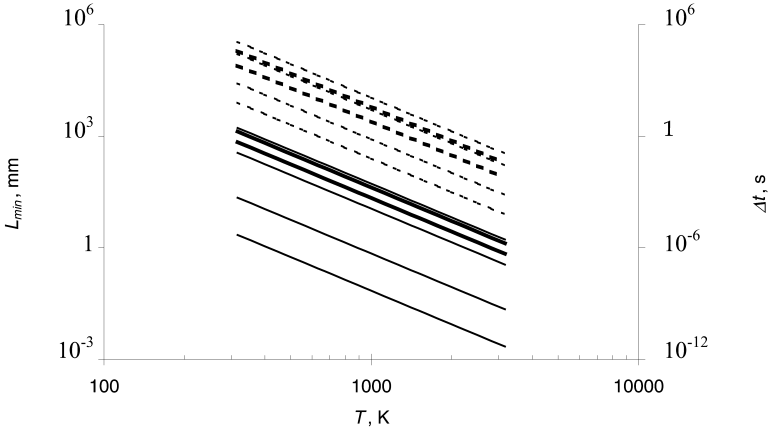


**Fig. 5.** Calculation of minimum sample size $L_{min}$ and measurement time $\Delta t$ for materials listed in Table I at different temperatures. Solid lines: with the left-hand scale from top to lower for Ta, W, Si, Fecr, Pyro, and BN. Dotted lines: with the right-hand scale from top to lower for Ta, W, Fecr, Si, Pyro, and BN.

recorded with a white card placed over the vacuum chamber window. After the card is removed and the shutter signal recorded for a few seconds, the furnace is lowered from its raised position (Fig. 4) and then the shutter withdraws at speed to expose the target (specimen or blackbody) for measurements. At each wavelength the signal-versus-time data can be fitted by the theoretical model to find the signal $S_0(\lambda)$ at $t = 0$, corresponding to the moment immediately before removal of the shutter when the target was isothermal and at a known temperature, $T_0$, as measured by thermocouples. Then the ratio of specimen to blackbody (BB) signal gives the spectral emissivity value. (Using Planck's law, the calculated emissivity value can be adjusted if necessary to compensate for any initial temperature difference between the specimen and blackbody.) The temperature of the BB also changes on exposure but at a much lower rate than a sample due to its large thermal mass and interior radiating area. However, the BB signal is obtained from data fitting to obtain the signal at time $t = 0$, just as for the sample.

### 4.3. Fecralloy Steel Measurements

A medium-ground Fecralloy steel of 10 mm diameter and 10 mm thick was chosen for measurement. Strictly, the sample radius is slightly smaller than the minimum size set by $L_{\min} = (10\alpha\, \Delta t)^{1/2}$. However, this will not raise a major difficulty in the measurement here because heat transfer at the sample surfaces, except the surface for measurement, is much reduced due to the sample being surrounded by the graphite sample block (Fig. 4).

Normal spectral emissivity measurements were made on the Fecralloy sample at temperatures of 683, 778, and 1073 K. Each measurement consists of 200 scans measured with the MCT detector during about 18 s over a wave-number range of 0 to 5000 $cm^{-1}$ (i.e., wavelength $\propto$ to 2 μm) with a resolution of 16 $cm^{-1}$. Each scan took about 90 ms during which the scanning time of the moving mirror in the FTS was about 60 ms, and the remaining 30 ms for data transfer and preparation for the next scan.

The measured spectral emissivity values are shown in Fig. 6. No significant change in the measured emissivity is observed with respect to temperature, which supports the assumption that temperature related emissivity changes are negligibly small.

### 4.4. Calculation of Hemispherical Total Emissivity

To calculate the hemispherical total emissivity $\varepsilon$ with Eq. (3), the specific time $t_0$ is required. The theoretical modeling in Section 2 showed that $t_0$ can be evaluated by fitting Eq. (6) to the measured spectral data.

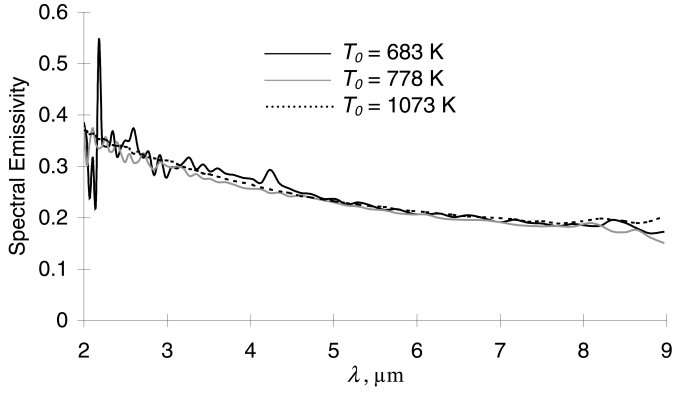


**Fig. 6.** Spectral emissivity measurements on a medium-ground Fecralloy steel at temperatures 683, 778, and 1073 K.

Figure 7 shows signals at wavelengths of 2, 3, and 4 μm, respectively, extracted from the measurement on Fecralloy at 1073 K, with their best-fit curves, each of which produces a value for $t_0$. The advantage of this approach to obtain $t_0$ is that the calculated $t_0$ values can be compared with each other to ensure consistency of total emissivity estimation with respect to wavelength $\lambda$.

It is assumed in the theoretical modeling that the spectral emissivity of the sample is unchanged during measurement, so the trace of surface temperature versus time can be calculated from spectral signals using Planck's law and the initial surface temperature $T_0$. Then an alternative approach to

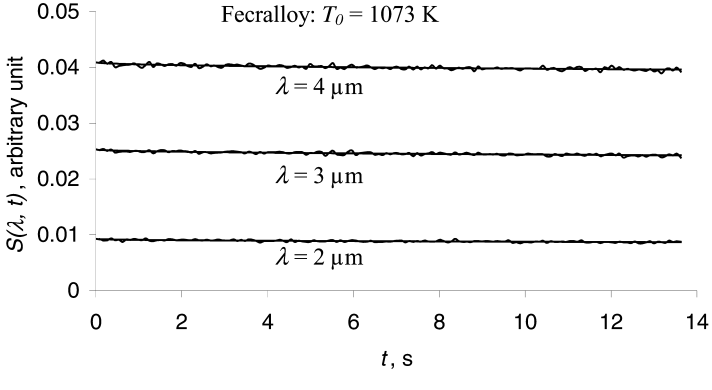


**Fig. 7.** Spectral signals measured from Fecralloy at $T = 1073$ K and wavelengths of 2, 3, and 4 μm. The smooth lines are their corresponding best-fit curves.

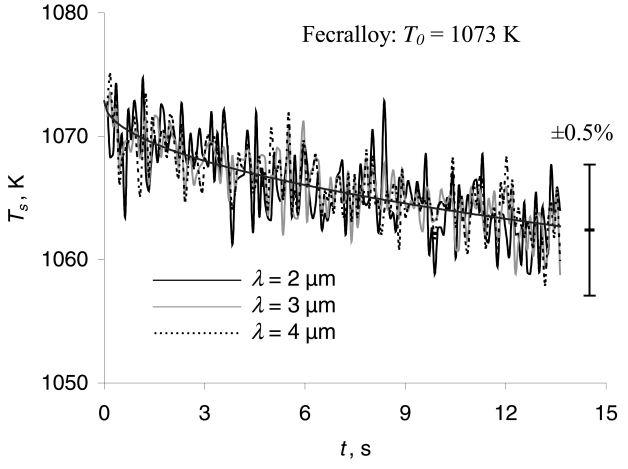


**Fig. 8.** Surface temperatures $T_S$ calculated from spectral signals measured at wavelengths of 2, 3, and 4 μm, respectively, for Fecralloy at an initial temperature of 1073 K. The smooth line is the best-fit curve.

obtain $t_0$ is to fit Eq. (2) to those surface temperatures. This alternative approach has two advantages: (i) the coefficients $a_n$ in Eq. (2) are independent of wavelength and (ii) $t_0$ can be calculated from measured signals at different wavelengths.

Figure 8 shows sample surface temperatures calculated using Planck's law from measured signals at wavelengths of 2, 3, and 4 μm for the Fecralloy sample at 1073 K. The temperature profiles are in agreement, which demonstrates consistency with respect to wavelength.

### 4.5. Comparing Hemispherical Total Emissivity Values

Figure 9 shows evaluated *hemispherical* total emissivity $\varepsilon$ values for the Fecralloy sample, in comparison with the *normal* total emissivity $\varepsilon_n$ value calculated by integrating measured normal spectral emissivity values between 2 and 9 μm. Ideally, the spectral measurements should be made over a wider range of wavelengths and angles to the surface and then integrated to give hemispherical total emissivity values. We adopted this comparison because there were no literature data for $\varepsilon$ of Fecralloy.

This could have led to a difference of up to 30% [10]. However, $\varepsilon$ values calculated from individual spectral signals between 2 and 4.5 μm (dots in Fig. 9) agree with each other to within 3%. Also shown in Fig. 9 is a single $\varepsilon$ value of 0.245 (solid line) obtained by fitting Eq. (2) to the

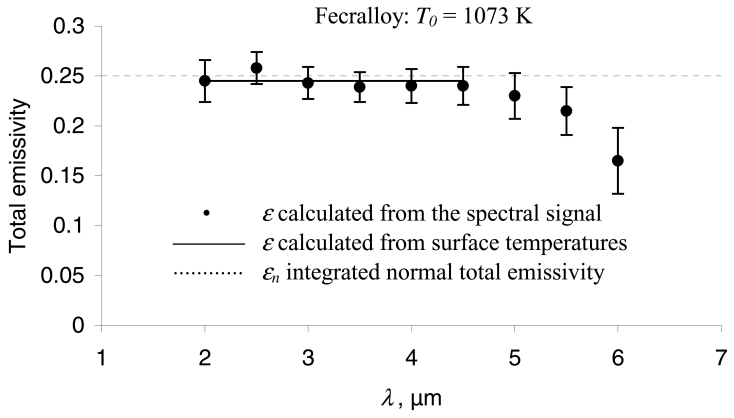


**Fig. 9.** Dots: hemispherical total emissivity $\varepsilon$ from fit to spectral signals between 2 and 4.5 μm. Solid line: $\varepsilon$ value from surface temperatures calculated from signals over 2 to 4.5 μm. Dotted line: the normal total emissivity $\varepsilon_n$ by integration of spectral emissivity values over 2 to 9 μm.

temperatures calculated from the signals measured between 2 and 4.5 μm. This latter $\varepsilon$ value is about 2% lower than 0.250, which is the $\varepsilon_n$ value estimated by integrating measured normal spectral emissivity values between 2 and 9 μm (dotted line in Fig. 9).

For $\lambda \geqslant 5$ μm, the estimated $\varepsilon$ values decrease with $\lambda$. This is probably due to the low signal-to-noise ratio (SNR) of signals at $\lambda \geqslant 5$ μm. The background radiation increases with wavelength, particularly for $\lambda \geqslant 5$ μm. However, the measured radiation decreases with wavelength due to the cut-off of the $CaF_2$ window at 9.6 μm and other optical components [7].

## 5. CONCLUSION

We have described a technique for estimation of hemispherical total emissivity values based on knowing the initial temperature and effusivity of a material, and compared it with total emissivity measurements derived from integration of normal spectral emissivity measurements. A theoretical model has been developed to study the temperature, heat flux and spectral radiation signals from a sample surface during a transient emissivity measurement. Calculations show that the temperature and heat flux decrease nonlinearly with measurement time, particularly at early time where the change rates can be high for materials of low effusivity and high emissivity. Therefore, measurement speed is important when considering the accuracy of the total emissivity determination.

The emissivity measurements on a sample of medium-ground Fecralloy steel show that calculated surface temperatures are consistent with respect to wavelength in the range 2 to 4.5 μm, and larger variation in the hemispherical total emissivity measured at longer wavelengths is believed due to the low SNR resulting from strong background radiation. The estimated hemispherical total emissivity obtained by the new approach is in good agreement with that obtained by integration of measured normal spectral emissivity values.

This is an early look at a novel method to obtain an independent check of the total emissivity value that is obtained by the new NPL emissometer. Further investigation is required to assess the new method for a wider range of materials and temperatures.

## APPENDIX A. SURFACE RADIATION FROM A SEMI-INFINITE SOLID

The temperature of a semi-infinite sample with surface radiation cooling to an environment at 0 K temperature has been studied by Jaeger [8]. In emissivity measurements, heat from the environment to the sample also needs to be considered with radiation heat loss at the sample surface. Using a similar mathematical treatment, and considering the initial condition and the heat flow continuity between thermal conduction inside the sample and radiation heat flux from its surface as described in Section 2, Eq. (1) can be solved to give

$$T(x, t) = T_0 + T_0 \sum_{n=1}^{\infty} \frac{2^n}{n!} a_n \Gamma\left(\frac{n}{2}+1\right)\left(\frac{t}{t_0}\right)^{\frac{n}{2}} i^n \operatorname{erfc} \frac{x}{\sqrt{4\alpha t}} \tag{A.1}$$

for $t > 0$, where $\Gamma$ is the Gamma function and $a_n$ is the $n$th coefficient, given by

$$a_1 = -1.1284u$$

$$a_2 = 8u$$

$$a_3 = -72.216u - 34.481u^2$$

$$a_4 = 768u + 1230.7u^2 + 91.673u^3$$

and so on, where $u = 1 - (\frac{T_a}{T_0})^4$.

The above derivation shows that, when $T_0 \gg T_a$, heat absorbed by the sample surface from the environment can be considered negligible in comparison with that radiated from the surface. Then $u = 1$ and $a_n$ become constants.

The surface temperature, $T_S(t)$ in Eq. (2) can be derived by setting $x = 0$ in Eq. (A.1) with [8]

$$i^n \operatorname{erfc} 0 = \frac{1}{2^n \Gamma(\frac{n}{2}+1)}$$

Coefficients $b_n$ in Eq. (4) can be calculated to give

$$b_1 = -4.5135u$$

$$b_2 = 32u + 15.279u^2$$

$$b_3 = -288.87u - 462.90u^2 - 34.481u^3$$

$$b_4 = 3072u + 11138u^2 + 3701.0u^3 + 38.908u^4$$

and so on. The above shows that, when $T_0 \gg T_a$ and then $u = 1$, $b_n$ become constants.

Coefficients $d_n$ in Eq. (6) for calculating spectral radiation signals can be evaluated by expanding Eq. (5) in the form of a Taylor series, to give

$$d_1 = \frac{B}{B-1} A a_1$$

$$d_2 = \frac{B^2+B}{(B-1)^2} A^2 a_1^2 - \frac{2B}{B-1} A a_1^2 + \frac{B}{B-1} A a_2$$

$$d_3 = \frac{B^3+4B^2+B}{(B-1)^3} A^3 a_1^3 + \frac{2B^2-6B}{(B-1)^2} A^2 a_1^3 + \frac{6B}{B-1} A a_1^3$$

$$+ \frac{3B^2+3B}{(B-1)^2} A^2 a_1 a_2 - \frac{6B}{B-1} A a_1 a_2 + \frac{B}{B-1} A a_3$$

and so on, where

$$A = \frac{C_2}{\lambda T_0} \qquad \text{and} \qquad B = e^{\frac{C_2}{\lambda T_0}}$$

## ACKNOWLEDGMENT

This work formed part of the UK's National Thermal Metrology Programme (2001–2004) managed by the National Measurement System Policy Unit of the Department of Trade & Industry.

## REFERENCES

1. Y. S. Touloukian and D. P. DeWitt, *Thermal Radiative Properties—Metallic Elements and Alloys, Thermophysical Properties of Matter*, Vol. 7 (IFI/Plenum, New York, Washington, 1970).
2. Y. S. Touloukian and D. P. DeWitt, *Thermal Radiative Properties—Non-Metallic Solids, Thermophysical Properties of Matter*, Vol. 8 (IFI/Plenum, New York, Washington, 1972).
3. M. J. Ballico and T. P. Jones, *Appl. Spectroscopy* **49**:335 (1995).
4. L. Werner, *Metrologia* **32**:531 (1995/1996).
5. S. Clausen, A. Morgenstjerne, and O. Rathmann, *Appl. Opt.* **35**:5683 (1996).
6. J. Redgrove, *High Temp.-High Press.* **17**:145 (1985).
7. B. Zhang, J. Redgrove, and J. Clark, presented at *The Sixteenth European Conference on Thermophysical Properties (ECTP)*, London (2002) and submitted to *High Temp.-High Press.*
8. J. C. Jaeger, *Proc. Camb. Philos. Soc.* **46**:634 (1950).
9. H. S. Carslaw and J. C. Jaeger, *Conduction of Heat in Solids*, 2nd edn. (Oxford University Press, London, 1959).
10. R. Siegel and J. R. Howell, *Thermal Radiation Heat Transfer*, 3rd edn. (Taylor & Francis, Washington, 1992), p. 122.